Manufacturing Letters xxx (xxxx) xxx

Contents lists available at ScienceDirect

Manufacturing Letters

journal homepage: www.elsevier.com/locate/mfglet

Metal structures embedded with piezoelectric PVDF sensors using ultrasonic additive manufacturing

Arun K. Ramanathan, M. Bryant Gingerich, Leon M. Headings, Marcelo J. Dapino *

NSF IUCRC on Smart Vehicle Concepts, Department of Mechanical and Aerospace Engineering, The Ohio State University, Columbus, OH 43210, USA

ARTICLE INFO

Article history:
Received 16 April 2021
Received in revised form 27 June 2021
Accepted 2 August 2021
Available online xxxx

Keywords:
Active metal structure
Embedded sensing
Ultrasonic additive manufacturing
Piezoelectric PVDF sensor
Non-destructive testing

ABSTRACT

Traditional manufacturing approaches to embed active materials, such as piezoelectrics, into metals can be problematic due to their high process temperatures or long curing times of the adhesives utilized to bond the active component to the metal. This paper presents the development and characterization of aluminum embedded with a piezoelectric polyvinylidene fluoride (PVDF) sensor using a low-temperature, solid-state metal joining process called ultrasonic additive manufacturing (UAM). The embedded sensor is subjected to a pre-compression that is empirically optimized by varying the depth of the pocket and tape foils welded above the sensor, thus eliminating reliance on a bonding medium to mechanically couple the metal and the sensor. The technology presented in this study could enable rapid fabrication of functionalized metal structures that can be used in non-destructive testing, energy harvesting, and load monitoring applications.

1. Introduction

Embedded sensors are expected to aid in digital manufacturing techniques for Industry 4.0 that require in-process monitoring and control techniques to optimize production time and cost by enabling realtime information retrieval [1,2]. Embedding sensors within a structure provides better proximity to the physical processes they monitor and also protects them structurally and thermally. In addition, it offers design freedom to optimize sensor location toward functionality with fewer manufacturing constraints.

Traditional embedding processes involve some form of high temperature melting and deposition to integrate the active material in a parent matrix [3–6]. These process temperatures generally exceed the Curie point of typical piezoelectric materials, leading to breakdown or deterioration of their sensing performance. In addition, the high process temperatures may also inflict damage to the associated electronics and wire cladding. Therefore, for diagnostics applications, piezoelectric sensors are fastened using rivets [7] or molded into structures using fiberglass [8], epoxy [9,10], silicone elastomer [11,12], or concrete [13]. In addition to the prohibitively long curing times required by epoxy or silicone mixtures to bond the sensor to metal, the presence of the bonding medium also influences the response of the embedded sensor [14].

Ultrasonic additive manufacturing (UAM) is a solid-state process that combines additive joining of metal foils and CNC–controlled milling operations to manufacture near-net shape metal components [15]. Ultrasonic vibrations generated by a rolling sonotrode, equipped with one or two piezoelectric transducers, are transmitted to the weld interface creating a low temperature, solid-state bond between the parts. The technology has been shown to successfully embed fiber-optic sensors [16,17], nickel-titanium (NiTi) shape memory alloy [18], printed electrical circuitry [19], and surface-mount resistors [20]. Some UAM processes combine ultrasonic welding with adhesive bonding [21] and low-pressure chemical vapor deposition [22] to embed sensors into metal structures.

Preliminary attempts demonstrated that the average temperature of the welding interface does not exceed the Curie temperature of PVDF, thus ensuring the electrical integrity of the sensor and its electroactivity after the welding process [15,23]. However, improvement to the embedment process, enhancement of mechanical coupling, and characterization of the active samples remain unexplored. This work focuses on the embedment of piezoelectric polyvinylidene fluoride (PVDF) sensors in an aluminum (Al) structure using UAM. Enhanced mechanical coupling is achieved through pre-compression of the sensor, which is specified by the depth of the milled pocket to effectively transfer strain to the sensor while avoiding damage during the UAM process. After

* Corresponding author.
E-mail addresses: ramanathan.38@osu.edu (A.K. Ramanathan), gingerich.37@osu.edu (M.B. Gingerich), headings.4@osu.edu (L.M. Headings), dapino.1@osu.edu (M.J. Dapino).

https://doi.org/10.1016/j.mfglet.2021.08.001
2213-8463/

developing a successful embedment procedure, the active specimen is subjected to quasistatic tensile tests and impulse compression tests to evaluate its electromechanical performance.

2. Sample fabrication

An embedment procedure as shown in Fig. 1(a) is carried out, wherein the piezoelectric sensor film is secured in the metalmatrix with the aid of a defined pre-compression applied by the layers welded on top of the film as shown in Fig. 1(b). A β-phase piezoelectric PVDF film coated with silver electrodes (TE Connectivity) is chosen as the piezoelectric material. Its relatively high piezoelectric voltage constant (g_{33}), mechanical compliance, and toughness makes it favorable for use with the UAM process. Polyimide tapes (Kapton) are chosen for lamination of the PVDF film to protect the film and its thin electrodes from the scrubbing action between the foil and material below it during ultrasonic welding [24] and to electrically insulate the electrodes from the bulk metal. Prior to embedding the actual PVDF sensor with its wire leads, an empirical approach is adopted to ensure feasibility of mechanically coupling the sensor and the metal-matrix by pre-compression while ensuring adequate metal-to-metal weld strength around the sensor. Based on visual inspection of the weld zones, pre-compression thicknesses up to 38 μm provided successful builds. Increasing the pre-compression further resulted in loss of weld strength and damaged the sensor. In consideration of the residual compressive stress and weld quality around the sensor, a 13 μm pre-compression of the embedded sensor is chosen for fabrication of a dogbone sample for testing. Details and figures related to the pre-compression identification process are provided in the supplementary document.

A PVDF sensor with wire leads is prepared as shown in Fig. 2(a). Copper tapes are attached to the sputtered silver electrodes of the poled PVDF film as shown in the inset of Fig. 2(a). Similar to the empirical study, the PVDF film is laminated with 50 μm thick polyimide (Kapton) sheets on either side, resulting in active sensor dimensions of 44 mm $\times$ 3.2 mm $\times$ 0.140 mm. Wires are then soldered onto the exposed regions of the copper leads and wrapped with electrical insulation tape. Fig. 2(a) shows a photograph of the PVDF sensor. Next, two Al foils are welded onto an Al 6061-T6 baseplate. Pockets for the PVDF sensor and its leads are machined as shown in Fig. 2(b). A sloped transition between the regions for the sensor and wire-sensor connections is provided to alleviate bending stress in the sensor during installation. The regions of the pockets milled for the soldered wire-sensor connections are deeper (600 μm) than the region for the sensor (510 μm), such that the pre-compression is applied only to the active sensing section of the PVDF sensor. The sensor is then positioned in the machined pocket and tacked in place as shown in Fig. 2(c). The sensor is verified to be above the metal surface using a depth gage. Finally, two Al 6061-T4 foils are ultrasonically welded on top of the baseplate as shown in Fig. 2(d). The welding parameters are chosen based on previous studies [25] and are listed in Table 1. The compression on the PVDF sensor is evident from the texture imparted to the foil by the sonotrode. This only occurs if there is an opposing force pushing the foil against the sonotrode. The welding zone is found to be free of any visual evidence of defects, the capacitance of the sensor is measured to be $C_S = 0.57$ nF, and its insulation resistance R_S is maintained above 100 MΩ, indicating that the electrodes are electrically insulated from each other and the Al matrix. The top foils are welded a few millimeters short of the end of the baseplate to provide an opening for the wires to

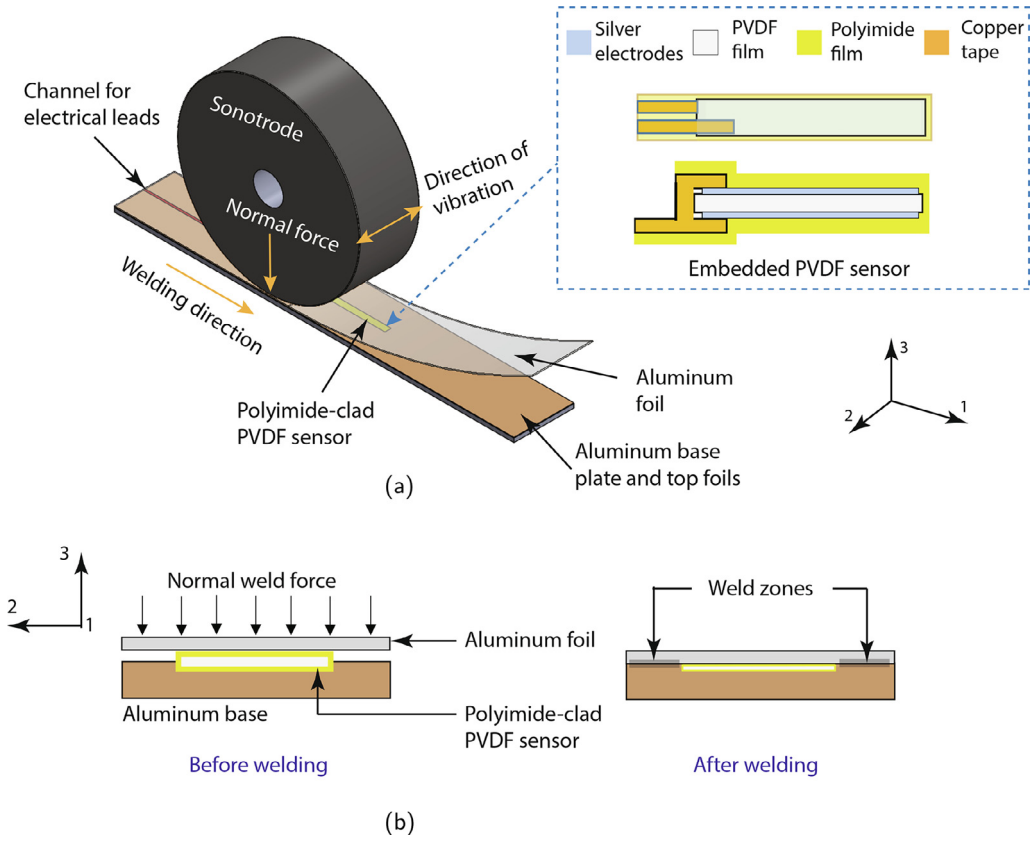

Fig. 1. (a) Illustration of an aluminum thin beam with an embedded piezoelectric PVDF sensor (inset) using ultrasonic additive manufacturing. (b) Cross-sectional illustration of the piezoelectric PVDF sensor subjected to compression during welding of the foil over the sensor.

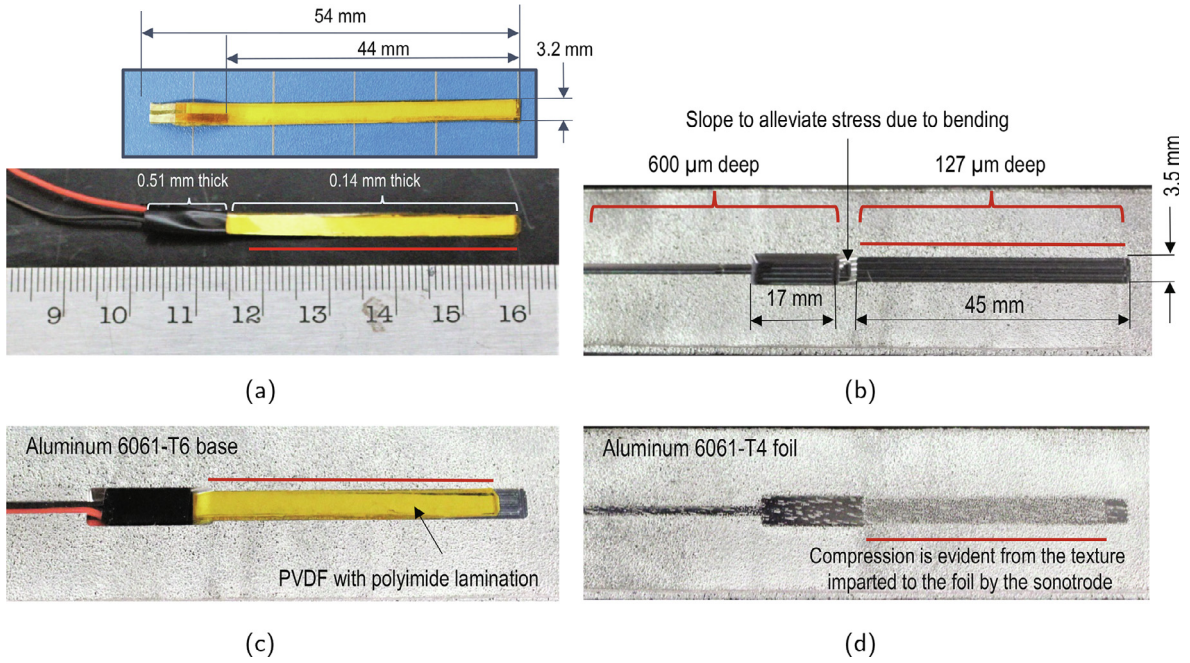

Fig. 2. Fabrication steps: (a) PVDF sensor with copper leads laminated with polyimide tapes (top); wires soldered onto the exposed portion of the copper leads and covered with electrical tape. The solid red line in each image represents the region subjected to compression during welding. (b) Pockets are milled in the baseplate for the PVDF sensor and the wires. (c) The sensor and the wires are secured in the machined pocket. (d) Two aluminum foil layers are ultrasonically welded on top of the sensor and the aluminum base.

Table 1
Process parameters used for the UAM build.

Parameters	Value
Thickness of the baseplate	2 mm
Thickness of the foil	0.152 mm
Thickness of PVDF sensor	40 μm
Thickness of polyimide film	2 × 50 μm
Weld (normal) force	4000 N
Weld amplitude	34 μm
Weld speed	42 mm/s
Sonotrode	uncoated (18Ni grade 350)
Temperature	23 °C

be folded out of the way to facilitate CNC milling of the dogbone-shaped (ASTM D638 Type I) specimen.

3. Experimental testing and results

The dogbone sample is subjected to a pre-defined sinusoidal tensile load profile on an MTS Criterion Model 43 load frame. The sample is tested below the yield limit of Al 6061-T6 (≈170 MPa) at its smallest cross-section, which corresponds to a maximum load of 4 kN at a sinusoidal frequency of 70 mHz. The specimen is subjected to a pretension of 100 N prior to the start of the test to prevent compression of the sample during the test cycle. The embedded sensor is interfaced through a near-static compensated charge amplifier with a gain S_{CA} of 0.01 mV/pC and lower cutoff frequency less than 0.01 mHz [26]. The output of the charge amplifier is connected to a National Instruments 9215 data acquisition module. The surface strain of the specimen is acquired every 0.2 s using a 5-megapixel Correlated Solutions VIC-3D digital image correlation (DIC) system [27] to correlate with the voltage measurements made by the embedded sensor.

Fig. 3(a) shows the strain field measured by the DIC system overlaid on a close-up photograph of the Al-PVDF specimen at the maximum applied load F_{max} of 4 kN. The solid black rectangle indicates the location of the embedded sensor and this area is utilized to compute the average tensile strain for each image. Fig. 3(b) shows that the measured PVDF voltage closely tracks the applied load in the time domain, indicating consistent strain-transfer from the Al-matrix to the PVDF sensor. This further indicates that there is adequate friction from pre-compression on the sensor to prevent slip between the sensor and the metal-matrix. A small voltage drift is observed in the measured voltage signal after connecting the PVDF sensor to the charge amplifier. This may be caused by a reduced insulation resistance of the PVDF sensor due to traces of electrically-conductive coolant, used in the machining process, present within the wiring channel leading to an impedance mismatch in the compensated charge amplifier [26]. However, the magnitude of the voltage drift is found to be only about 2% of the total amplitude at the end of one test cycle. This is not large enough to interfere with the characterization experiments and can be removed in post-processing.

Fig. 3(c) shows the voltage measured from the embedded PVDF sensor versus average tensile strain in the marked sensor area in Fig. 3(a) for three consecutive trials. The embedded sensor exhibits excellent linearity ($R^2 > 0.99$) and repeatability within the investigated load range *and test cycles.* Based on a similar study performed for characterizing the fatigue performance of a fiber Bragg grating (FBG) sensor using UAM, the samples tested provided reliable measurements for up to 9500 cycles and only deteriorated after the Al CT samples failed [17]. However, a detailed study is warranted to establish the fatigue performance of the presented device for different load cycles and at elevated temperatures. The mean strain sensitivity S_V of the embedded sensor interfaced with the charge amplifier is measured to be 53.8 $\mu V\ \mu\varepsilon^{-1}$. This corresponds to a quasistatic open-circuit sensitivity $S_\varepsilon = S_V/(C_S S_{CA}) = 9.4$ mV $\mu\varepsilon^{-1}$, where C_S is the capacitance of the PVDF sensor.

Finally, assuming uniaxial tension, the average tensile stress in the PVDF film is calculated from the measured voltage V_M as [28]

$$T_{1S,avg} = \frac{Q}{d_{31} A_S} = \frac{V_M}{S_{CA} d_{31} A_S}, \quad (1)$$

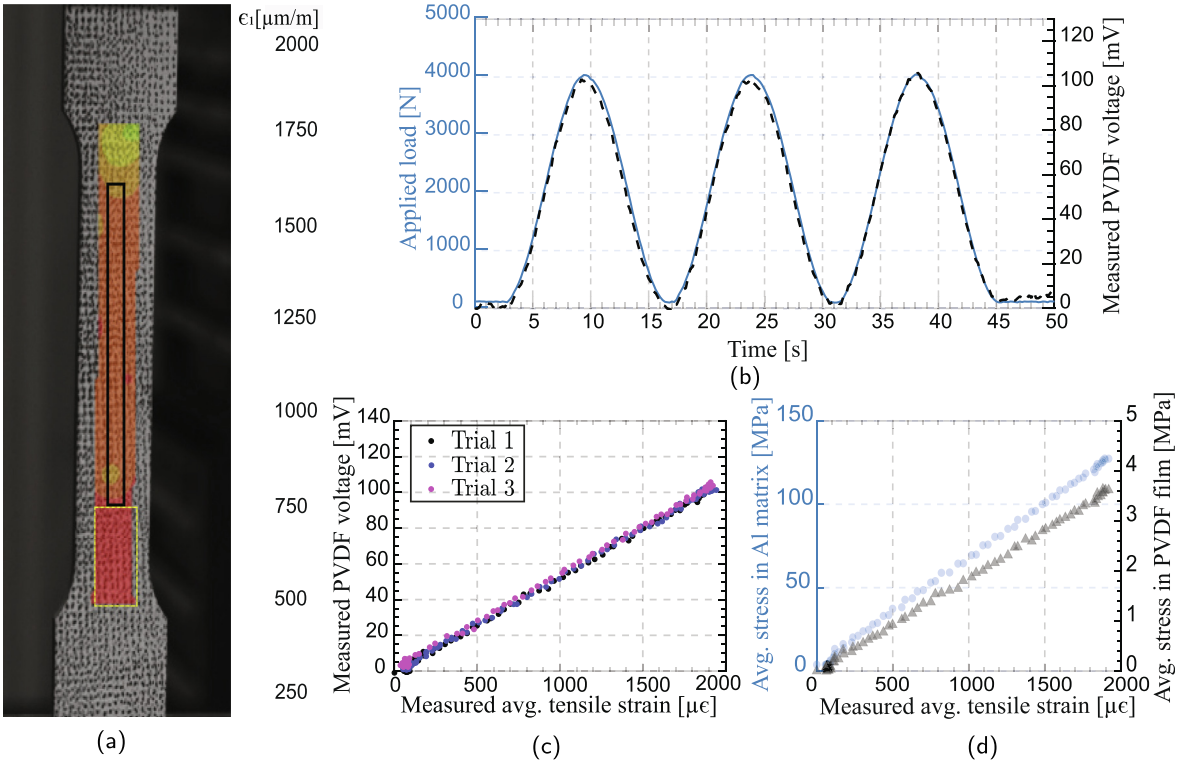

Fig. 3. Tensile testing of the Al-PVDF structure: (a) Strain field captured by the DIC system at the maximum applied load of 4 kN. The solid black rectangle indicates the location of the embedded PVDF sensor and the yellow dashed region indicates the location of the lowest cross-sectional area in the specimen. (b) Applied load vs. quasi-static PVDF voltage tracked in the time domain for three consecutive load cycles. (c) Voltage measured from the embedded PVDF sensor vs. average tensile strain of the sensor area indicated in (a). (d) Average stress in the specimen and average stress in the PVDF vs. average tensile strain. Average stress in the PVDF film is computed from the measured voltage.

where Q is the charge output due to the applied strain, d_{31} is the piezoelectric stress constant, and A_S is the electrode area. The average tensile stress in the specimen is given as

$$T_{1C,avg} = \frac{F}{A_C}, \tag{2}$$

where A_C is the cross-sectional area of the aluminum bulk. Using the two equations above, the average tensile strain versus the average tensile stress in the aluminum and the average stress in the PVDF film is shown in Fig. 3(d). The maximum average tensile stress in the PVDF film is observed to be lower than its yield strength of 35 MPa. Neglecting the Poisson effect, for complete strain transfer under uniaxial loading, the stiffness ratio between aluminum and PVDF is

$$\gamma = \frac{E_{Al}}{E_S} = \frac{T_{1C,avg}}{T_{1S,avg}}. \tag{3}$$

Using $E_{Al} = 68.9$ GPa, the ratio of the elastic modulus of Al to the elastic modulus of PVDF is calculated to be 27.5. However, the ratio of the slopes of the two plots in Fig. 3(d) is $\gamma = 32.2$, which is 14.5% higher than the estimate, indicating a possible loss of strain. However, sensor slip or decoupling would have resulted in hysteresis, inconsistent voltage output, or loss of linearity from the embedded sensor during tensile testing. Since no such discrepancies are observed in the voltage output, the loss of strain can be attributed to the compliance of the interlayer. The fidelity of the present model could be improved by considering the properties of the interlayer to calculate an effective strain transfer ratio [29]. Nevertheless, an empirically calibrated strain or load sensitivity of the active specimen is useful for most non-destructive testing (NDT) and load sensing applications. In addition, the Al-PVDF specimen is also subjected to compressive (g_{33}) impulse loads to evaluate its impact detection, frequency bandwidth, and localization performance. The results of the above test are provided in the supplementary document.

4. Concluding remarks

This article presents a rapid fabrication procedure for embedding a piezoelectric PVDF sensor in an aluminum matrix using a low-temperature UAM process that creates a defined pre-compression of the sensor within the host material to enhance the mechanical coupling. The active specimen demonstrated a mean open-circuit sensitivity of 9.4 mV $\mu\varepsilon^{-1}$ under uniaxial tension with excellent linearity. Apart from the strain and impact detection capabilities of the Al-PVDF specimen presented in this article, the proposed fabrication process could be effectively utilized toward rapid fabrication of functionalized metal structures for use in thermal measurements, energy harvesting, and structural health monitoring applications.

Declaration of Competing Interest

The authors declare that they have no known competing financial interests or personal relationships that could have influenced the work reported in this paper.

Acknowledgements

Financial support was provided by the member organizations of the Smart Vehicle Concepts Center, a Phase III National Science Foundation Industry-University Cooperative Research Center (www.SmartVehicleCenter.org) under grant NSF IIP 1738723.

Appendix A. Supplementary data

Supplementary data associated with this article can be found, in the online version, at https://doi.org/10.1016/j.mfglet.2021.08.001.

References

[1] Shaffer D, Ragai I, Danesh-Yazdi A, Loker D. Investigation of the feasibility of using microphone arrays in monitoring machining conditions. Manuf Lett 2018;15:132–4.
[2] Kumar A. Methods and materials for smart manufacturing: additive manufacturing, internet of things, flexible sensors and soft robotics. Manuf Lett 2018;15:122–5.
[3] Juhasz M, Tiedemann R, Dumstorff G, Walker J, Du Plessis A, Conner B, Lang W, MacDonald E. Hybrid directed energy deposition for fabricating metal structures with embedded sensors. Addit Manuf 2020;35:101397.
[4] Hossain MS, Gonzalez JA, Hernandez RM, Shuvo MAI, Mireles J, Choudhuri A, Lin Y, Wicker RB. Fabrication of smart parts using powder bed fusion additive manufacturing technology. Addit Manuf 2016;10:58–66.
[5] Li X, Golnas A, Prinz FB. Shape deposition manufacturing of smart metallic structures with embedded sensors. Smart Structures and Materials 2000: Sensory Phenomena and Measurement Instrumentation for Smart Structures and Materials, volume 3986. International Society for Optics and Photonics; 2000. p. 160–71.
[6] Petrat T, Kersting R, Graf B, Rethmeier M. Embedding electronics into additive manufactured components using laser metal deposition and selective laser melting. Procedia CIRP 2018;74:168–71.
[7] Ihn J-B, Chang F-K. Detection and monitoring of hidden fatigue crack growth using a built-in piezoelectric sensor/actuator network: II. Validation using riveted joints and repair patches. Smart Mater Struct 2004;13:621.
[8] Schulze R, Streit P, Fischer T, Tsapkolenko A, Heinrich M, Sborikas M, et al., Fiber-reinforced composite structures with embedded piezoelectric sensors, in: SENSORS, 2014 IEEE, IEEE, 2014, pp. 1563–1566.
[9] Park J-M, Kong J-W, Kim D-S, Yoon D-J. Nondestructive damage detection and interfacial evaluation of single-fibers/epoxy composites using PZT, PVDF and P (VDF-TrFE) copolymer sensors. Compos Sci Technol 2005;65:241–56.
[10] Caneva C, De Rosa I, Sarasini F. Monitoring of impacted aramid-reinforced composites by embedded PVDF acoustic emission sensors. Strain 2008;44:308–16.
[11] Acer M, Salerno M, Agbeviade K, Paik J. Development and characterization of silicone embedded distributed piezoelectric sensors for contact detection. Smart Mater Struct 2015;24:075030.
[12] Sonar HA, Paik J. Soft pneumatic actuator skin with piezoelectric sensors for vibrotactile feedback. Front Robot AI 2016;2:38.
[13] Liu T, Zou D, Du C, Wang Y. Influence of axial loads on the health monitoring of concrete structures using embedded piezoelectric transducers. Struct Health Monitor 2017;16:202–14.
[14] Han L, Wang X, Sun Y. The effect of bonding layer properties on the dynamic behaviour of surface-bonded piezoelectric sensors. Int J Solids Struct 2008;45:5599–612.
[15] Wolcott P, Dapino M. Ultrasonic additive manufacturing. In: Badiru A, editor. 3D Printing Handbook: Product Development for the Defense Industry. p. 275–313.
[16] Hehr A, Norfolk M, Kominsky D, Boulanger A, Davis M, Boulware P. Smart build-plate for metal additive manufacturing processes. Sensors 2020;20:360.
[17] Chilelli SK, Schomer JJ, Dapino MJ. Detection of crack initiation and growth using fiber bragg grating sensors embedded into metal structures through ultrasonic additive manufacturing. Sensors 2019;19:4917.
[18] Hahnlen R, Dapino MJ. NiTi-Al interface strength in ultrasonic additive manufacturing composites. Compos Part B 2014;59:101–8.
[19] Li J, Monaghan T, Nguyen T, Kay R, Friel R, Harris R. Multifunctional metal matrix composites with embedded printed electrical materials fabricated by ultrasonic additive manufacturing. Compos Part B 2017;113:342–54.
[20] Bournias-Varotsis A, Han X, Harris RA, Engstrøm DS. Ultrasonic additive manufacturing using feedstock with build-in circuitry for 3D metal embedded electronics. Addit Manuf 2019;29:100799.
[21] Siggard EJ, Madhusoodanan AS, Stucker B, Eames B. Structurally embedded electrical systems using ultrasonic consolidation (UC). In: 2006 International solid freeform fabrication symposium. p. 308–16.
[22] Cheng X, Datta A, Choi H, Zhang X, Li X. Study on embedding and integration of microsensors into metal structures for manufacturing applications. J Manuf Sci Eng 2006;129:416–24.
[23] R. Hahnlen, M.J. Dapino, Active metal-matrix composites with embedded smart materials by ultrasonic additive manufacturing, in: Industrial and commercial applications of smart structures technologies 2010, vol. 7645, International Society for Optics and Photonics, 2010, p. 764500.
[24] Han T, Kuo C-H, Sridharan N, Headings LM, Babu SS, Dapino MJ. Effect of weld power and interfacial temperature on mechanical strength and microstructure of carbon steel 4130 fabricated by ultrasonic additive manufacturing. Manuf Lett 2020;25:64–9.
[25] Wolcott PJ, Hehr A, Dapino MJ. Optimized welding parameters for Al 6061 ultrasonic additive manufactured structures. J Mater Res 2014;29:2055–65.
[26] Chillara V, Ramanathan A, Dapino M. Self-sensing piezoelectric bistable laminates for morphing structures. Smart Mater Struct 2020;29:085008.
[27] Schreier H, Orteu J-J, Sutton MA, et al. Image correlation for shape, motion and deformation measurements: Basic concepts, theory and applications, volume 1. Springer; 2009.
[28] Leo DJ. Engineering analysis of smart material systems. John Wiley & Sons; 2007.
[29] Li H-N, Zhou G-D, Ren L, Li D-S. Strain transfer coefficient analyses for embedded fiber Bragg grating sensors in different host materials. J Eng Mech 2009;135:1343–53.

Arun Kumar Ramanathan received his B.E. degree in Automobile Engineering from Anna University, Chennai, India, in 2012 and his M.Sc. degree in Mechanical Engineering from The Ohio State University, USA, in 2017. He is currently pursuing his Ph.D. in Mechanical Engineering under the supervision of Prof. Marcelo Dapino at The Ohio State University, USA. His research interests include design, characterization, and fabrication of flexible sensors for vehicle applications.

M. Bryant Gingerich worked as a research associate in the Department of Mechanical and Aerospace Engineering at The Ohio State University until July 2020. He earned his M.S and B.S in mechanical engineering from The Ohio State University, graduating in 2016. His research specializations are in Ultrasonic Additive Manufacturing, joining systems, and automotive structural design. He now works as the owner and founder of Dunlap Hollow LLC in Rockbridge, Ohio.

Leon M. Headings is a senior research associate in the Department of Mechanical and Aerospace Engineering at The Ohio State University. He earned his Ph.D., M.S., and B.S. in mechanical engineering from The Ohio State University and his B.A. in physics from Goshen College. Prior to his graduate work, he worked his passenger and light truck tire development at Bridgestone Americas, Inc. His research interests include the modeling, characterization, development, and control of smart material devices and advanced manufacturing systems.

Marcelo J. Dapino is a professor in the Department of Mechanical and Aerospace Engineering at The Ohio State University, where he is the Honda R&D Americas Designated Chair in Engineering and Director of the Smart Vehicle Concepts Center, a National Science Foundation Industry-University Cooperative Research Center. Prof. Dapino received his Ph.D. degree from Iowa State University and his Engineering Diploma from the University of Uruguay. His research interests include smart materials and structures, advanced manufacturing, and dynamic systems.